Analytical Model for Hook Anchor Pull-Out

Brincker, Rune; Ulfkjær, Jens Peder; Adamsen, Peter; Langvad, Lotte; Toft, Rune

Published in:
Proceedings of the International Symposium on Anchors in Theory and Practice

Publication date:
1995

Document Version
Publisher's PDF, also known as Version of record

PROCEEDINGS OF THE INTERNATIONAL SYMPOSIUM ON ANCHORS IN THEORY AND PRACTICE / SALZBURG / AUSTRIA / 9-10 OCTOBER 1995
BERICHTE DES INTERNATIONALEN SYMPOSIUMS ANKER IN THEORIE UND PRAXIS SALZBURG / ÖSTERREICH / 9.-10. OKTOBER 1995

Anchors in Theory and Practice
Anker in Theorie und Praxis

Editor / Herausgeber
RICHARD WIDMANN
Österreichische Gesellschaft für Geomechanik

OFFPRINT/SONDERDRUCK

A.A. BALKEMA / ROTTERDAM / BROOKFIELD / 1995

Anchors in Theory and Practice, Widmann (ed.) © 1995 Balkema, Rotterdam. ISBN 90 5410 577 1

Analytical model for hook anchor pull-out

Analytisches Modell für die Haftfestigkeit von Ankern mit Querplatte

Rune Brincker, Jens Peder Ulfkjær, Peter Adamsen, Lotte Langvad & Rune Toft
University of Aalborg, Denmark

ABSTRACT: A simple analytical model for the pull-out of a hook anchor is presented. The model is based on a simplified version of the fictitious crack model. It is assumed that the fracture process is the pull-off of a cone shaped concrete part, simplifying the problem by assuming pure rigid body motions allowing elastic deformations only in a layer between the pull-out cone and the concrete base. The derived model is in good agreement with experimental results, it predicts size effects and the model parameters found by calibration of the model on experimental data are in good agreement with what should be expected.

ZUSAMMENFASSUNG: Ein einfaches analytisches Modell für die Haftfestigkeit von Anker mit Querplatte ist behandelt. Das Modell basiert sich auf eine vereinfachte Fassung des fiktiven Riss modells. In diesem Modell wird angenommen, dass die Materialpunkte am Rissverlängerungspfad sich in einem der folgenden möglichen Stadien befinden: A) lineärelastisches Stadium, B) Riss stadium, wo das Material durch Kohäsionskräfte in der Riss prozesszone erweichert ist, und zuletzt C) ein Stadium mit keine Spannungstransmission. Im Bruchstadium ist der Riss prozess von einer erweicherten Relation beschrieben, die die Normalspannungen der Bruchfläche σ mit der Rissöffnung, w (Abstand zwischen die Bruchflächen) verbindet. Es wird angenommen, dass der Bruchform eine Entziehung eines kegelförmigen Betonkörpers entspricht. Das Problem wird vereinfacht durch die Annahme, dass reine Steifkörperbewegungen nur elastische Deformationen in einer Schicht zwischen den Haftfestigkeitskegel und das Betonbasis erlauben. Die steuerenden Gleichungen werden dann mittels einfachen Gleichgewichtsbedingungen abgeleitet. Das abgeleitete Modell stimmt mit den experimentellen Resultaten gut überein. Es kann Gröss eneffekte voraussagen, und die Modellparameter, die durch kalibrierung des experimentellen Datenmodells mit experimentellen Daten gefunden ist, stimmen mit den Erwartungen gutüberein.

1 INTRODUCTION

Anchors are used in most reinforced concrete structures. It might be simple adhesive anchors, expansion anchors or hook anchors, figure 1. Usually, the simple adhesive anchor, figure 1.a is used where it is possible. It is simple and reliable. Further, since this anchor is usually designed in such a way that the load bearing capacity of the adhesive anchor relies on the shear resistance of the interface between the bar and the concrete, the failure process is ductile, and thus, as for all ductile failure problems, no or at least small size effects are observed. However, the simple adhesion anchor needs a relatively long embedment length to ensure enough load bearing capacity, and to ensure that the failure of the anchor will be pull-out of the anchor bar. If the space is limited and the embedment length is reduced, there is a risk that the mode of failure will change from pull-out of the bar to pull-off of a concrete cone. In this case, the failure is more brittle, and the load-bearing capacity no longer depends on the shear resistance of the interface. In this case, the load-bearing capacity depends on the tensile strength and the fracture energy of the concrete material and of the size and the shape of the pulled-off concrete cone. The bigger the cone, the larger the load-bearing capacity, and, thus, it is natural to force the concrete cone to start as deeply as possible. This can be done by introducing an expansion part at the end of the anchor, figure 1.b, but the safest way of ensuring the cone to start at the end of the anchor is to provide the anchor with a "hook", usually shaped like an anchor plate at the end of thenchor bar, figure 1.c. As already mentioned, since the failure of the hook anchor mostly

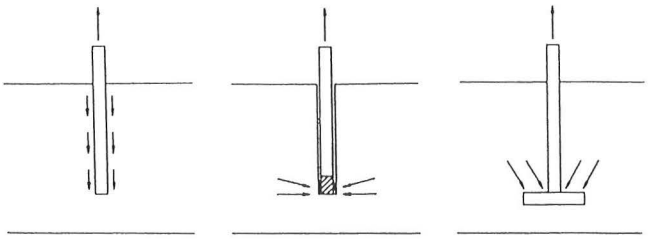

Figure 1. Different ways of transferring the load from the anchor bolt to the concrete, a) adhesive anchor, b) expansion anchor and c) hook anchor.

Figur 1: Verschiedene Methoden für Lasttransmission von Kopfbolzendübel zu Beton, a) Klebeanker, b) Expansionsanker und c) Anker mit Querplatte.

depends on the fracture mechanical properties of the concrete, the load-bearing capacity is expected to show a clear size effect.These size effects have been observed by several researchers, Bocca et al. 1990, and by Eligehausen and Savade ,1989. Their results indicate a strong size effect over embedment depth ranging from 50 mm to 500 mm. Eligehausen and Clausnitzer,1983, studied the behaviour of anchors by finite element models. Their investigation showed a clear influence of the type of model used. An ideal plastic model gave higher load-bearing capacities than a more brittle model using material softening.

Elfgren et al. ,1987, also studied the problem numerically using a fictitious crack model approach for the softening material. Their investigation indicates, that the shear stresses in the crack should be incorporated in the model. Also Rots,1990, investigated the problem numerically. He studied the influence of the number of radial cracks (cracking of the concrete cone) and used a smeared crack approach. His results indicate that the number of radial cracks tend to increase the ultimate load. Elfgren and Ohlson ,1990, studied the influence of tensile strength and fracture energy using a finite element analysis. As expected, their results indicate that the ultimate load and the ductility of the failure process increase with the fracture energy, and that increasing the tensile strength will increase the ultimate load and the brittleness of the failure process. Bocca et al. ,1990, made an analysis using the fictitious crack model in a finite element analysis using axi-symmetric elements and a re-meshing technique. They found good agreement with experimental results. Also Ozbolt and Eligehausen,1993, made a finite element analysis using axi-symmetric elements. They showed that cracking starts at about 30 % of the ultimate load, and that the ultimate load is mainly determined by the fracture energy. Also, their results indicate a strong size effect on the ultimate load.

Tommaso et al. ,1993, investigated the influence of the shape of the crack opening relation. They found that a bi-linear softening curve predicts more realistic results than a single-linear curve. Similar results have been found by Urchida et al. ,1993.

2 BASIC ASUMPTIONS

In this section the basic assumptions of the simplified model describing anchorage pull-out using the fictitious crack approach is presented. The fictitious crack model is due to Hillerborg, 1977, but the basic idea is close to that of Dugdale, 1960, who used a similar approach assuming a constant yield stress in the fracture zone, and Barenblatt, 1962, who assumed a more general distribution of the stresses in the fracture zone. Usually the fictitious crack model concept is used in finite element programs using special no-volume elements, 1989, or using the smeared crack approach Rots 1989, or it might be formulated using sub-elements describing the elastic behaviour and introducing the softening only for the material in the pre-selected crack path, Petersson, 1982, Brincker and Dahl, 1989. However, these methods are complicated and time-consuming to use for design, and they do not provide simple analytical solutions indicating the degree of brittleness and indicating how strongly a certain problem might be influenced by size effects. Thus, it is desirable to have simple models that describe the basic fracture behaviour qualitatively correct in order to have simple tools especially for

describing the brittleness of the failure process.

The intention of the models presented here is to formulate the simplest possible model that reflects the basic fracture mechanical behaviour. The model problem is illustrated in figure 2. The problem is assumed to be plane, i.e. the 3-dimensional problem is not considered, and thus radial crack are omitted from the analysis. Further, the crack path is assumed to be linear, the slope being described by the angle φ, and the deformation is assumed to be a rigid body motion as a rotation around the point where the crack path meets the surface of the concrete. The depth L is related to the radius of the cone by the equation $L = R \tan(\varphi)$. The cone and the surrounding concrete is assumed to be perfectly rigid, all the elasticity being described by an elastic layer between the cone and the rest of the body. This simple approach has proved its value in modelling of the failure process for plain and reinforced beams, Ulfkjær et al. 1993a, 1993b, 1995.

In the distance r from the edge of the anchor stud the vertical deformation w is

$$w = u\left(1 - \frac{r}{R}\right) \tag{1}$$

This deformation will cause vertical as well as horizontal stresses in the elastic layer, and horizontal as well as vertical reactions at the rotation point. However, in this simplified analysis, it will be assumed, that the geometry is chosen in such a way, that the vertical reactions at the rotation point can be neglected. Thus, considering only vertical stresses $\sigma = \sigma(r)$, the corresponding force is given by

$$F = \int_0^R 2\pi r \sigma(r)\, dr \tag{2}$$

3 SINGLE-LINEAR SOFTENING

For the case of single-linear softening the physical relation of the layer is as shown in figure 3, i.e. the elastic part is linear and the softening part is linear. Here w is the the total deformation and, thus, it includes elastic as well as softening terms.

For any point in the crack path, as long as the stresses have not reached the ultimate stress σ_u, the response is linear, and no crack is present at that point. The deformation w_u where the softening starts is given by

$$w_u = \delta \frac{\sigma_u}{E} \tag{3}$$

where E is Young's modulus of the concrete, and δ is the thickness of the elastic layer. eq. (3) defines the layer thickness δ.

The fracture energy is the area below the stress-deformation relation in figure 3, i.e. the fracture energy is

$$G_F = \frac{1}{2} w_c \sigma_u \tag{4}$$

Using the introduced physical relation for the elastic layer the stress is given by

$$\sigma(r) = \begin{cases} w(r)\dfrac{\sigma_u}{w_u} & \text{for } w(r) \le w_u \\ \sigma_u \left(1 - w(r) - \dfrac{w_u}{w_c} - w_u\right) & \text{for } w_u \le w(r) \le \\ 0 & \text{for } w_c \le w(r) \end{cases} \tag{5}$$

As it appears, this divides the fracture process into three phases. In phase I the deformation u has not reached the deformation w_u and thus, no fictitious

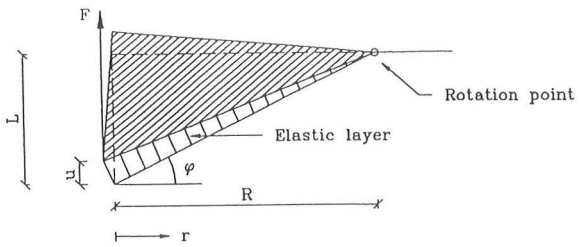

Figure 2. Geometry of simplified fictitious crack model.

Figur 2: Geometrie des vereinfachten fiktiven Riss modells.

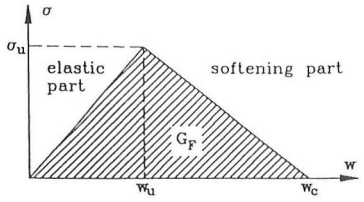

Figure 3. Stress-deformation relationship for the case of single-linear softening.

Figur 3: Spannungs-Deformationsverhältnis für monolineare Erweicherung.

crack is present. In phase II u is between w_u and w_c, i.e. a fictitious crack has developed. Finally, in phase III u has exceeded the critical crack opening w_c and a real crack has developed. The stress distributions for the three phases are illustrated in figure 4. Let c denote the length of the real crack, and let a denote the total length of the crack (real crack + fictitious crack). Now, using eq. (1) and (2) together with eq. (5) and carrying out the integrations, the following expression is obtained for the force

$$F = 2\pi\sigma_u\left(\frac{1}{2}(a^2-c^2)\left(1-\frac{u-w_u}{w_c-w_u}\right) + \frac{1}{3}(a^3-c^3)\frac{u}{R}(w_c-w_u)\right) + 2\pi\frac{\sigma_u}{w_u}u\left(\frac{1}{6}R^2+a^2\left(\frac{a}{3}R-\frac{1}{2}\right)\right) \quad (6)$$

where the crack parameters a and c are given by

$$a = \begin{cases} 0 & \text{for } u<w_u \\ R(1-w_u/u) & \text{for } u\geq w_u \end{cases} \quad (7)$$

$$c = \begin{cases} 0 & \text{for } u<w_c \\ R(1-w_c/u) & \text{for } u\geq w_c \end{cases} \quad (8)$$

The equations (6), (7) and (8) describe the pull-out of the concrete cone using the displacement u as the controlling parameter. To use the model the constitutive parameters σ_u, w_u and w_c most be known as well as the radius R of the cone at the concrete surface. Figure 5 shows a typical load-displacement curve simulated by the model using the values $R = 1000w_c$, $w_u = 2/17\ w_c$ and $G_F = 178\ \sigma_u/w_c$ The plot was made non-dimensional by dividing the force F by $\sigma_u R^2$ and the displacements u by w_c.

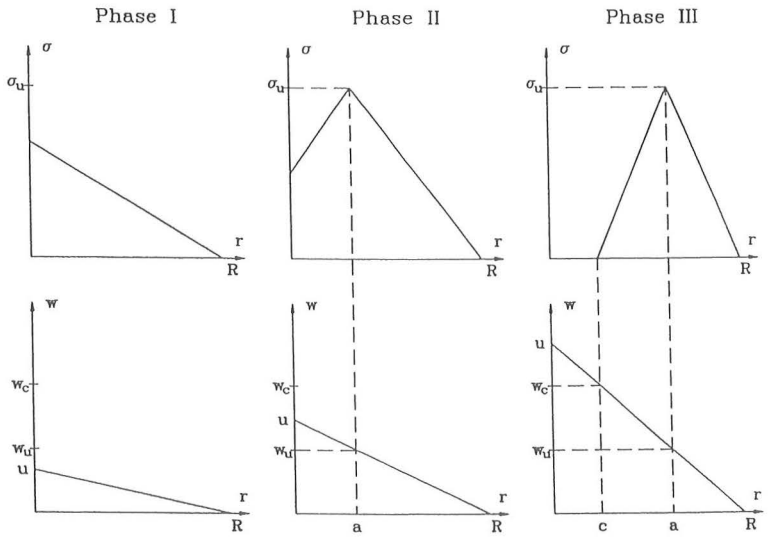

Figure 4. Stress distribution in the three phases.

Figur 4. Spannungfeld für die drei stadien

Figure 5. Relati

Figur 5: Kraft-I

4 BRITTLENE

The introduced a
of expressing th
The classical bri
1989, might be d
the fracture of
definition

$$B = 2\frac{w_u}{w_c}$$

using this defi
yields the follc
number for the

$$B = \frac{w_u\sigma_u}{G_F} = \frac{\delta\sigma}{EG}$$

In this express
the ultimate st
strength f_t of
elastic layer m
S of the rel

ıing.

c are given by

(7)

(8)

ribe the pull-out of
lacement u as the
the model the
w_c most be known
ne at the concrete
load-displacement
ng the values R =
σ_u/w_c The plot was
he force F by $\sigma_u R^2$

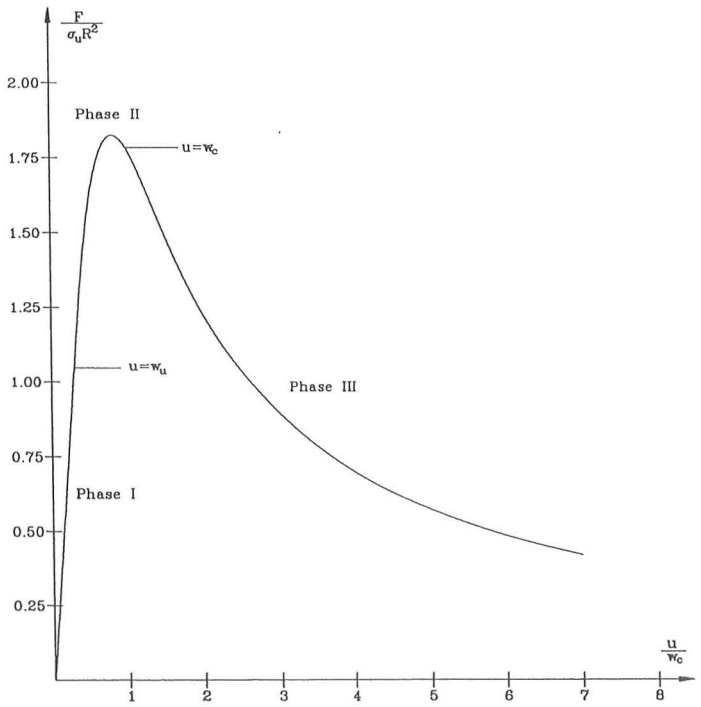

Figure 5. Relationship between force and deformation simulated by the model using single-linear softening.

Figur 5: Kraft-Deformationsverhältnis simuliert mittels monolinearer Erweicherung.

4 BRITTLENESS AND SIZE EFFECTS

The introduced analytical model provide a simple way of expressing the brittleness of the pull-out problem. The classical brittleness number $B = f_t^2\, l/EG_F$ Bache , 1989, might be derived from the single-linear model of the fracture of a bar in uniaxial tension using the definition

$$B = 2\frac{w_u}{w_c} \tag{9}$$

using this definition together with eqs. (3) and (4) yields the following expressions for the brittleness number for the pull-out problem

$$B = \frac{w_u \sigma_u}{G_F} = \frac{\delta \sigma_u^2}{EG_F} \tag{10}$$

In this expression it would be natural to assume that the ultimate stress σ_u is proportional to the tensile strength f_t of the concrete. The thickness δ of the elastic layer might be estimated from the initial slope S of the relation between the force F and the displacement u at the bottom plate. From the elastic regime of eq. (6) or (11) the relation is found as $\delta = \pi R^2 E/3S$. The shape of the pull-out relation depends on the brittleness number B. This effect is illustrated in figure 6 showing results for the single-linear case.

By introducing the brittleness number into equation (6), (7) and (8) and making all quantities non-dimensional the following simplfied equations are obtained

$$\frac{\mu}{2\pi\sigma_u L^2} = \frac{1}{2}(\alpha^2 - \gamma^2)\left(1 - \frac{\theta - 1}{\frac{2}{B} - 1}\right) + \frac{1}{3}(\alpha^3 - \gamma^3)\frac{\theta}{\rho\left(\frac{2}{B} - 1\right)} + \theta\left(\frac{1}{6}\rho^2 + \alpha^2\left(\frac{\alpha}{\rho} - \frac{1}{2}\right)\right) \tag{11}$$

where the crack parameters α and γ are given by

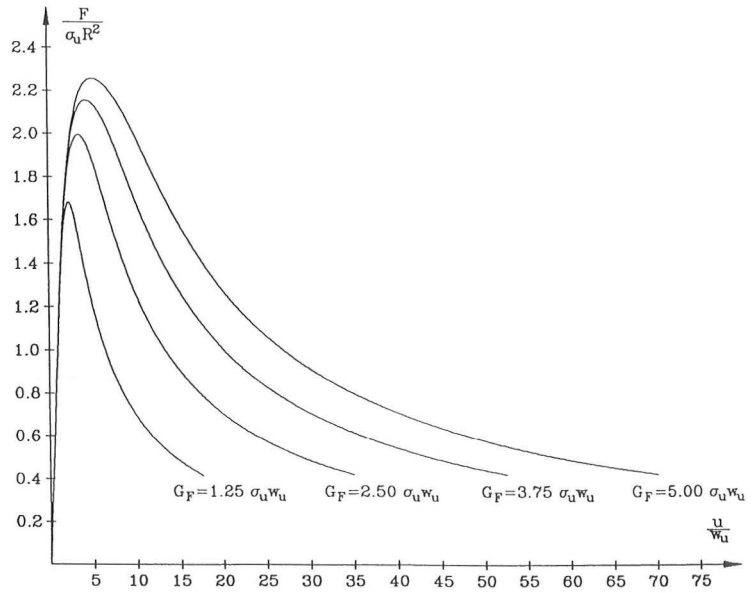

Figure 6. Influence of the brittlenes number B illustrated by varying the fracture energy G_F.

Figur 6: Einfluss von Sprödigkeitszahl B illustriert durch varierende Bruchenergie G_F.

$$\alpha = \begin{cases} 0 & \text{for} \quad \theta < 1 \\ \rho\left(1 - \frac{2}{\theta}\right) & \text{for} \quad \theta \geq 1 \end{cases} \tag{12}$$

$$\gamma = \begin{cases} 0 & \text{for} \quad \theta < \frac{2}{B} \\ \rho\left(1 - \frac{2}{B\theta}\right) & \text{for} \quad \theta \geq \frac{2}{B} \end{cases} \tag{13}$$

where $\theta = u/w_u$ is the controlling parameter and $\rho = R/L$ is a shape parameter. By writing the problem in non-dimensional form it ts seen that the problem is completely described by the brittleness number B and the shape parameter ρ simplifing the problem considerrably.

Size effects are studied by varying the size of the pull-out problem considering geometrically similar cases and comparing the ultimate load F_u normalised by $\sigma_u L^2$ corresponding to the normalization in equation (11). The result is shown in figure 7. The maximum size effect that can be predicted by the model is found using the stress distributions $\sigma = \sigma_u$ corresponding to ideal ductile behaviour (very small sizes) and $\sigma = \sigma_u(R-r)/R$ corresponding to brittle behaviour (large sizes). Using these stress distributions in eq. (2) it is found that the maximum size effect predicted by the model is a factor of three - exactly the same as for a beam in bending, Ulfkjær et al., 1995. Note, that since the linear fracture mechanics is not incorporated in this model, no size effects are predicted when the size exceeds a certain level. This model predicts only the non-linear size effects, i.e. the size effects in the region where non-linear effects are dominating. In cases where the non-linear effects are not dominating, i.e. for very large specimens, using the results of the analysis carried out here might be misleading. However, the analysis indicates, figure 7, that for small embedment depths, for L ranging from 0 to about 50 mm, non-linear effects are dominating, and thus, the results predicted by the model should be representative.

5 EXPERIMENTS

In order to investigate the aplicability of the derived model a series of experiments with high strength concrete is performed.

5.1 *Specimens*

The specimens were rectangular with a depth of 150 mm and base
mm by 620 mm
the anchor.
between 25 mm
tested.

5.2 *Concrete*

A high strengt
The composi
The cylinde
splitting stre
determined u
mm cylinders
840 mm by
notch was sa
beams were
physical para
2.

5.3 *Casting*

All the spec
was delive
facturer. Th

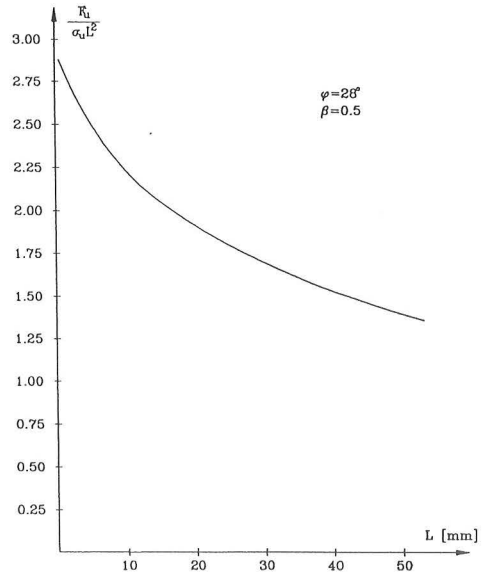

Figure 7. Model predicted size effects on the load-bearing capacity.

Figur 7: Modellierte Gröss eneffekte auf der Tragfähigkeit.

mm and base of either 1120 mm by 1120 mm or 620 mm by 620 mm dependent on the embedment depth of the anchor. The embedment depths were varied between 25 mm and 95 mm. In all 18 specimens were tested.

5.2 *Concrete*

A high strength concrete was used for the experiments. The composition of the concrete is shown in table 1. The cylinder compressive strength, the cylinder splitting strength and the modulus of elasticity were determined using standard methods on 100 mm by 200 mm cylinders. The fracture energy was determined on 840 mm by 100 mm by 100 mm beams in witch a notch was saw cut at the mid-section of the beam. The beams were subjected to three point bending. The physical parameters of the concrete are shown in table 2.

5.3 *Casting*

All the specimens were casted of the same batch, wich was delivered from a commercial concrete manufacturer. The anchor was embedded in the middle of the concrete matrix. The load was apllied at an anchor stud. The diameter of the anchor stud was 18 mm, the diameter of the anchor head was 34 mm and the thichkness of the head was 25 mm. On top of the anchor head an anchor extension with a diameter of 8 mm was mounted. The extension was so long so it would reach the opsite side of the speciemen. The anchor extension was used to measure the displacements of the anchor. The same dimension were used for all the anchors.

5.4 *Test Set-up*

The test set-up and geometri is shown in figure 8. The anchor is pulled out by downwards movement of the piston, which is linked to the anchor stud by an adaptor. At the top of the test specimen an LVDT (Linear Variable Differential Transformer) is situated. The LVDT meassures the vertical displacement of the bottom of the anchor head via the the extension mountet on the anchor head. Since the fitting for the LVDT is fixed at the concrete plate, deflection of the plate has no effect on the meassurements of the LVDT.

The above mentioned placing of the LVDT has been chosen because the displacement of the piston was not

Table 1. Composition of concrete.

Component	Amount [kg/m^3]
Cement	445
Silica	35
Gravel	881
Sand	822
Water	147
Peramin F (Plast.)	4.2
Pozz 80 (Super Plast)	0.7

Table 2. Physical parameters of the concrete

Property	Value
Modulus of Elasticity	39.6 GPa
Compressive strength	87.6 MPa
Splitting Strength	5.3 MPa
Fracture Energy	o.o93 N/mm

found suitable for estimating the movement of the anchor. This is due to friction between the anchor and the concrete, deformations of the test rig, elastic deformations of the test specimen and local crushing of the concrete. All thses phenomenon makes it impossible to correct for false deformations. In figure 9 is shown the difference between the piston deformation and the LVDT. Comparing the load displacement history of the piston and the LVDT a large difference is seen. This supports the importance of the method of the direct meassurements of the displacement of the anchor.

A servocontrolled material testing sysstem is used. Both the LVDT and the piston displacement isincluded in the feedback signal which controls the movements of the piston. The feedback signal is created by analog addition of the corresponding signals from the piston and the LVDT in the following proportion:

$$U_f = 0.9U_{LVDT} + 0.1U_{PISTON} \quad (14)$$

where U_f is the feedback signal, U_{LVDT} is the signal from the LVDT and U_{PISTON} is the signal from the piston.

6 CALIBRATION AND EVALUATION

The model was calibrated on the 18 pull-out tests. The calibration was performed by inspecting the fit visually using a computer programme allowing for easy adjustment of all relevant parameters. Figure 10 shows the result of a typical calibration. As it appears, the fit is quite good over the entire measurement range.

The parameters were calibrated in the following way. First, the stress σ_u was chosen as a fixed value close to the measured tensile strength of the concrete. Then the initial slope was calibrated as explained in the preceding section. Then the peak load and peak deformation were calibrated by simultaneously changing the the radius R and the fracture energy G_F. A better estimate of the parameters can however be obtained by using an automized optimization algorithm as done for beams in three point bending in Ulfkjær and Brincker, 1992.

The results of the calibrations are shown in table 1. As it appears, two values are given for the radius, the value R for the final radius observed after the test, and the effective radius R' as it was estimated by calibration of the model, figure 11. As it appears, typically there is a factor 2-3 between the two values.

Amount [kg/m³]
445
35
881
822
147
4.2
0.7

Value
39.6 GPa
87.6 MPa
5.3 MPa
o.o93 N/mm

JATION

pull-out tests. The
:ting the fit visually
llowing for easy
s. Figure 10 shows
s it appears, the fit
rement range.

:he following way.
xed value close to
:oncrete. Then the
explained in the
: load and peak
simultaneously
acture energy G_F.
s can however be
ed optimization
: point bending in

shown in table 1.
or the radius, the
after the test, and
is estimated by
. As it appears,
n the two values.

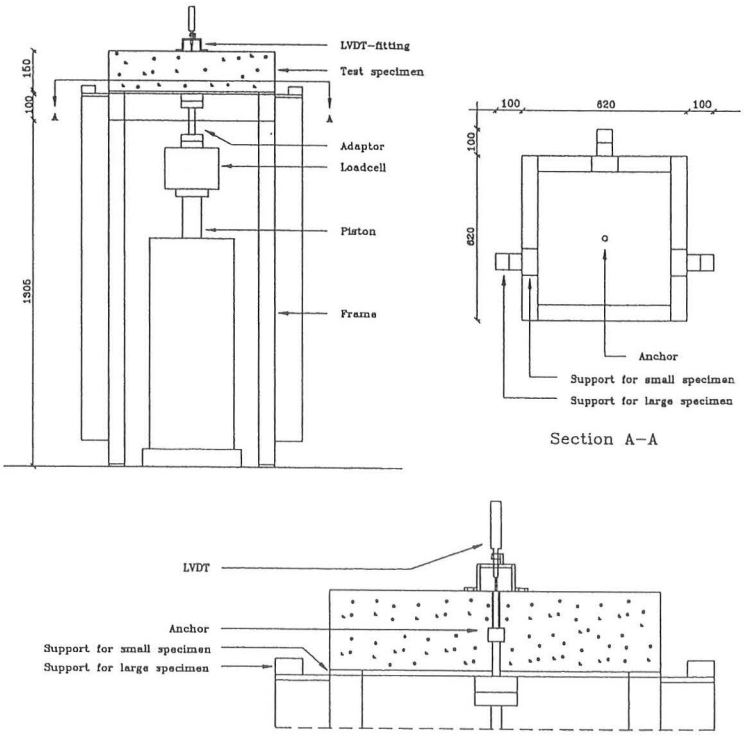

Figure 8. The test set-up

Figur 8. Die Versuchsaufstellung.

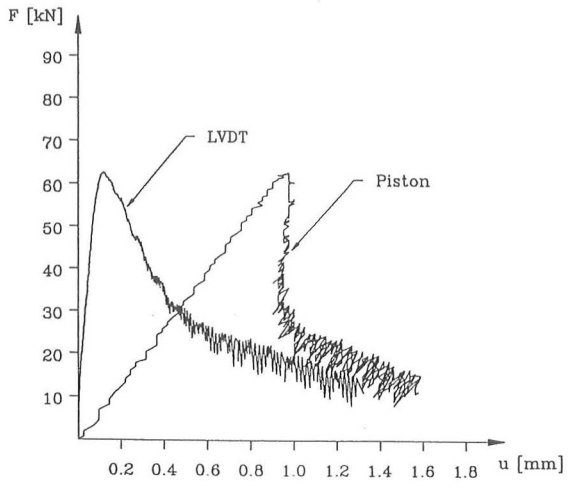

Figure 9. Force versus displacement. Displacement of piston and meassured by LVDT.

Figur 9. Kraft gegen Bewegen. Das Bewegen des Kolben und gemessen von LVDT.

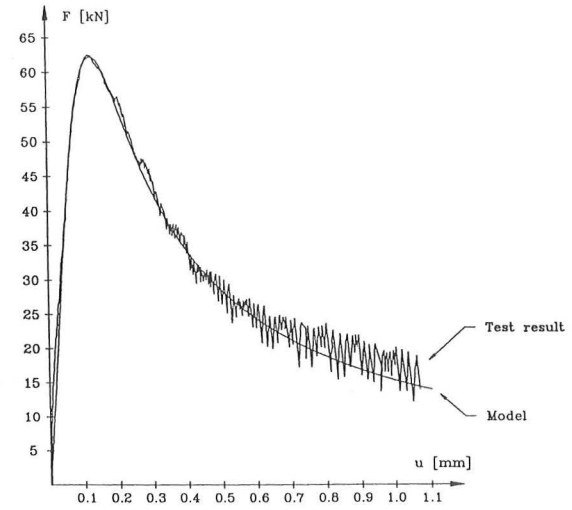

Figure 10. Calibration of model to test result.

Figur 10: Kalibrierung des Modells zu Testresultaten.

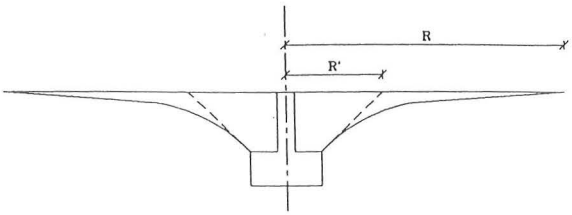

Figure 11. Radius R observed by test, and effective radius R' used in model.

Figur 11: Radius R gefunden im Test, und effektiver Radius R' benutzt im Modell.

The results do not necessarily represent any serious discrepancy between the model and reality. The cones that were pulled off during the test showed a curved crack path corresponding to large initial values of φ that were substantially decreased during the fracture process. Thus, since the model include only one value of φ, and since this value should be close to the initial value of φ observed during the test, relatively small values of the radius R should be expected when calibrating the model.

Further, the values of the fracture energy estimated by the model, the effective fracture energy G'_F, is substantially larger than usual fracture energies for concrete. Since an ordinary high-strength concrete was used, this effect must be due to the model. However, as before, this is to be expected considering the low values of the effective radius R'. Since the area under the force-displacement curve is approximately correct, the following relationship between the real and the effective parameters must hold $\pi R'^2 G'_F = \pi R^2 G_F$. If the values of the effective fracture energy is interpreted in this way, the results become close to the values of the fracture energy usually observed experimentally.

An examination of the estimated values for the effective radius R' and for the initial angle φ indicates that the problem is not geometrically independent of the size. Figure 12 shows the estimated values of φ as a function of the size. As it appears, the fracture angle does not seem to be constant. The results indicate a typical value of φ around 20-25 degrees for very small embedment depths, and a value of φ around 40 degrees for embedment length around 100 mm.

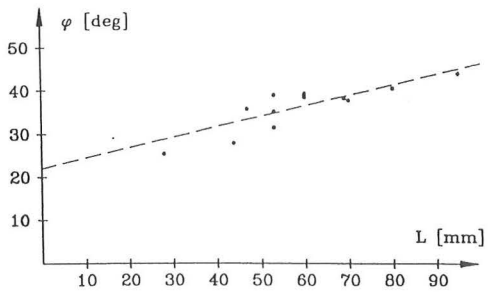

Figure 12. Estimated fracture angle φ as a function of the embedment depth.

Figur 12: Estimierter Bruchwinkel φ als Funktion der Haftstrecke.

Table 3. Model parameters estimated by calibration of the model

Name	L	R'	R	σ_b	G_F	φ
28 a	28	59	125	5.0	0.45	25.4
44 a	44	83	235	5.0	0.38	27.9
47 a	47	65	225	5.0	0.55	35.9
47 b	47	65	205	5.0	0.55	35.9
47 c	47	65	190	5.0	0.55	35.9
53 b	53	75	220	5.0	0.40	35.3
53 c	53	65	265	5.0	0.72	39.1
55 b	53	86	185	5.0	0.35	31.6
60 a	60	73	255	5.0	0.50	39.4
60 b	60	75	240	5.0	0.68	38.6
69 b	69	87	255	5.0	0.50	38.4
69 c	69	87	260	5.0	0.50	38.4
70 a	70	90	265	5.0	0.50	37.9
70 c	70	90	280	5.0	0.60	37.9
80 c	80	93	190	5.0	0.50	40.7
95 b	95	98	200	5.0	0.42	44.1

7 CONCLUSIONS

A simple model has been presented for the non-linear fracture mechanical problem of the pull-out of a concrete cone in a hook anchor failure test.

The model is formulated combining the fictitious crack model with very simple assumptions concerning the displacement field and the elastic response of the material around the crack path. Further, the solutions only correspond to an approximate satisfaction of the equilibrium equations.

To investigate the applicability of the model 18 pull

out tests were performed on a high strength concrete. In order to investigat size effects different embedment depths were studied. The experiments showed a significant size effect compared to codes.

The model was calibrated to the pull-out tests in different sizes. The model gave a fine fit to the experimentally measured pull-out curves, and the estimated model parameters correspond well to what should be expected.

8 RÉFERENCES

Bache, H., 1989: Brittleness/Ductility from a Deformation and Ductility points of View, in L. Elfgren (ed.) Fracture Mechanics of Concrete Structures, Chapman and Hall, pp. 202-207.

Barenblatt, G.I, 1962., in H.L. Dryden and T. Karman (eds.), pp. 56-131 : Advances in Applied Mechanics, Academic, Vol. 7.

Brincker, R and H. Dahl, 1989: On the Fictitious Crack Model of Concrete Fracture, Magazine of Concrete Research, Vol. 41, No. 147, pp. 79-86.

Bocca, P., A. Carpinteri and S. Valente, 1990: Fracture Mechanics Evaluation of Anchorage Bearing Capacity in Concrete}, Applications of Fracture Mechanics to Reinforced Concrete, Ed. A. Carpinteri, Elsevier Applied Science, pp. 231-265}

Dugdale, D.S, 1960.: Yielding of Steel Sheets Containing Slits, Journal Mech. Phys. Solids, Vol. 8, pp. 100-104.

Elfgren, L., U. Ohlson and K. Gylltoft, 1987: Anchor Bolts Analysed with Fracture Mechanics, Proc. of the International Conference on Concrete and Rock, Houston, Texas, June 17-19.

Elfgren, L., and U. Ohlson, 1990: Anchor Bolts Modelled with Fracture Mechanics, Applications of Fracture Mechanics to Reinforced Concrete, Ed. A. Carpinteri, Elsevier Applied Science, pp. 231-265.

Eligehausen, R. and Clausnitzer, 1983: Analytiches Modell zur Bescreibung des Tragverhaltens von Befestigungselementen, Report 4/1-83/3, Institut fü Werstoffe im Bauwesen, Universität Stuttgart.

Eligehausen, R. and G. Savade, 1989: A Fracture Mechanics based Description of the Pull-Out Behaviour of Headed Studs Embedded in Concrete, Ed. L. Elfgren, RILEM Report, Chapman and Hall, pp. 264-280.

Hillerborg, A., M. Modeer and P.E. Petersson, 1977: Analysis of Crack Formation and Crack Growth in Concrete by Means of Fracture Mechanics and Finite Elements, Cement and Concrete Research, Vol. 6, No. 6, Nov..

Hillerborg, A. and J.G. Rots, 1989: Crack Concepts and Numerical Modelling pp. 128-137 in L. Elfgren (ed.) Fracture Mechanics of Concrete Structures, Chapman and Hall.

Ozbolt, R. and Eligehausen, 1993: Fastening Elements in Concrete Structures, Fracture and Damage of Concrete and Rock, Ed. H.P. Rossmanith, Proc. of the 2nd International Conference on Fracture and Damage of Concrete and Rock, Vienna, Austria, E & FN Spon.

Petersson, P.E.: Crack Growth and Development of Fracture Zones in Concrete and Similar Materials, Report TVBM-1006, Division of Building Materials, Lund Institute of Technology, Sweden.

Rots, J.G, 1989.: Smeared Crack Approach, in L. Elfgren (ed.) Fracture Mechanics of Concrete Structures, Chapman and Hall, pp. 138-146.

Rots, J.G., 1990: Simulation of Bond and Anchorage: Usefulness of Softening Fracture Mechanics, Applications of Fracture Mechanics to Reinforced Concrete, Ed. A. Carpinteri, Elsevier Applied Science, pp. 231-265.

Tomasso, A.D., O. Manfrodi and G. Valente, 1993: Comparison of Finite Element Concrete Models Simulating Pull-Out Tests, Fracture and Damage of Concrete and Rock, Ed. H.P. Rossmanith, Proc. of the 2nd International Conference on Fracture and Damage of Concrete and Rock, Vienna, Austria, E & FN Spon.

Uchida, Y., K. Rokugo and W. Koyanagi, 1993: Numerical Analysis of Anchor Bolts Embedded in Concrete Plates, Fracture and Damage of Concrete and Rock, Ed. H.P. Rossmanith, Proc. of the 2nd International Conference on Fracture and Damage of Concrete and Rock, Vienna, Austria, E & FN Spon.

Ulfkjær, J.P. and Brincker R. 1992, Indirect Determination of the σ-w Relation of HSC through Three-Point Bending, Concrete and Rock Rossmanith), Vienna, pp.135-144.

Ulfkjær, J.P., O. Hed 1993a: Simple Applic in Reinforced Concre Symposium on Fr Materials, Concrete, F Australia.

Ulfkjær, J.P., O. Hec 1993b: Simple Appli in Reinforced Con Experiment, Proc. of on size Effects in co

Ulfjkær, J.P., S. K Analytical Model fo Concrete Beams, Jo Vol. 121, No. 1.

Three-Point Bending, in Fracture and Damage of Concrete and Rock, FDCR-2 (Edited by H.P. Rossmanith), Vienna, Austria, E & FN Spon, London, pp.135-144.

Ulfkjær, J.P., O. Hededal, I. Kroon and R. Brincker, 1993a: Simple Applications of Fictitious Crack Model in Reinforced Concrete Beams, Proc. of the IUTAM Symposium on Fracture of Brittle Disordered Materials, Concrete, Rock and Ceramics, Queensland, Australia.

Ulfkjær, J.P., O. Hededal, I. Kroon and R. Brincker, 1993b: Simple Application of Fictitious Crack Model in Reinforced Concrete beams - Analysis and Experiment, Proc. of the JCI International Workshop on size Effects in concrete Structures, Sendai, Japan.

Ulfjkær, J.P., S. Krenk and R. Brincker, 1995: Analytical Model for Fictitious Crack Propagation in Concrete Beams, Journal of Engineering Mechanics, Vol. 121, No. 1.

FROM THE SAME PUBLISHER:

Bui, H.D. & M.Tanaka (eds.) 90 5410 517 8
Inverse problems in engineering mechanics – *Proceedings of the 2nd international symposium, Paris, 2-4 November 1994*
1994, 25 cm, 492 pp., Hfl.185 / $110.00 / £69
Many inverse problems of great practical importance are found in engineering mechanics alone, and there is currently a dramatic increase of research activity in this area. This book contains about 65 selected papers by authors from Europe, Asia and America. The overall contents reflect the state of the art in this particular applied research area. The main topics are: Unknown shape determination; Identification of material properties; System determination; Boundary conditions and source identification; Defect identification; Mathematical and computational aspects; Experimental strategy.

Chambon, R., J.Desrues & I.Vardoulakis (eds.) 90 5410 511 9
Localisation and bifurcation theory for soils and rocks
Proceedings of the 3rd Workshop, Grenoble, France, 6-9.09.1993
1994, 25 cm, 288 pp., Hfl.150 / $90.00 / £56
Localisation and other related instability phenomena are known to play a crucial role in the ultimate behaviour of soils and rocks at and during rupture and constitute the basis of a continuum theory of rupture. Proper modelling of strain localisation and other bifurcation phenomena can be very significant in several fields, among which one can cite: Environmental engineering & disaster prevention; Slope stability analysis, monotonous and cyclic behaviour, liquefaction phenomena; Petroleum engineering: Borehole stability, sand production, drilling; Mining industry: Rock bursting, tunnel instability; Civil engineering: Stability of foundations, embankments, excavations, retaining walls and Powder & Grains engineering: Storage and controlled flow of granular masses.

Lancellotta, R. 90 5410 178 4
Geotechnical engineering
April 1995, 25 cm, c.400 pp., Hfl.190 / $95.00 / £70
(Student edn., 90 5410 179 2, Hfl.115 / $60.00 / £43)
This book is about the mechanics of soils and structures interacting with soils, based on the material collected at the Technical University of Turin over the past two decades. *Contents:* Nature and composition of soils; The principle of effective stress and the state variables; Fundamentals of continuum mechanics; The porous medium: steady flow; The porous medium: transient flow; Stress-strain and strength characteristics; In-situ investigations; The collapse of soil structures; Performance and serviceability of structures; References; Index. Author: Technical University of Turin, Italy.

Hustrulid, W. & M.Kuchta (eds.) 90 5410 173 3
Fundamentals of open pit mine planning and design
May 1995, 25 cm, c.850 pp., 2 vols, Hfl.245 / $125.00 / £90
(Student edn., 90 5410 183 0, 2 vols, Hfl.125 / $65.00 / £46)
The books is divided into two parts. Part 1 consists of six chapters in which the basic planning & design principles are presented: Mine planning; Mine revenues & costs; Orebody description; Geometrical considerations; Pit limits; Production planning. Much of the actual calculation involved in the design of an open pit mine is done by computer. Two professional computer programs CSMine & VarioC have been specifically developed with the university undergraduate learning environment in mind. These programs, their related tutorials & user manuals, together with a data set for the CSMine Property, are subject of part 2 of this book. Six chapters involved are: Introduction; CSMine property description; CSMine tutorial; CSMine user's manual; VarioC tutorial & user's guide; VarioC reference manual.

Xie, Heping (M.A.Kwasniewski, Editor-in-Chief) 90 5410 133 4
Fractals in rock mechanics (Geomechanics Research Series, 1)
1993, 25 cm, 464 pp., Hfl.150 / $85.00 / £55
Important developments in the progress of the theory of rock mechanics during recent years are based on fractals and damage mechanics. The book is concerned with these developments, as related to fractal descriptions of fragmentations, damage, and fracture in rocks, rock bursts, joint roughness, rock porosity and permeability, rock grain growth, rock and soil particles, shear slips, fluid flow through jointed rocks, faults, earthquake clustering, etc. A simple account of the basic concepts, methods of fractal geometry & their applications to rock mechanics, geology & seismology. Discussion of damage mechanics of rocks & its application to mining engineering. Author: China Univ. of Mining & Technology, Xuzhou, China.

Andreev, G.E. 90 5410 602 6
Brittle failure of rock materials
Tests results and constitutive models
March 1995, 25 cm, c.380 pp., Hfl.195 / $115.00 / £74
Comprises different basic aspects of brittle failure for rocks. Classical & contemporary models are considered theoretically as well as failure patterns under different loading schemes. Terminology; Strength theories; Contemporary models about brittle fracture; Laborational methods for determining some mechanical properties of rocks; Mohr strength envelopes; Experimental investigation of brittle behaviour; Size effect; Concluding remarks and references.

Saxena, K.R. 90 5410 278 0
Geotechnical engineering: *Emerging trends in design and practice*
1994, 25 cm, 410 pp., Hfl.105 / $60.00 / £39 (No rights India)
New approaches & state-of-the-art reports on sampling disturbance & application of numerical models, study of swelling characteristics of deep residual clays, cemented marine carbonate soils, constitutive models & geotechnical applications, control of uncertainty, determination of design parameters, embankment dam & earthquakes, machine foundations, design & construction of tailings dams, geosynthetics in embankment dams & as material for soil reinforcement.

Bräuner, Gerhard 90 5410 158 X
Rockbursts in coal mines and their prevention
1994, 25 cm, 152 pp., Hfl.120 / $70.00 / £44
The preventive methods desribed have proved highly effective. They comprise laying out the workings in such a way as to minimize dangerous concentrations of ground stresses, and early elimination by means of blasting, drilling, or water infusion. An account of these methods as applied in German coal mines, the deepest in the world. *Contents:* Rockbursts & similar phenomena; Conditions of occurrence; Influence of rock stress; Bursting & nonbursting coal; Long-term prevention; Direct prevention; Borehole patterns for direct prevention; Destressing methods; Case histories. Author: formerly Deutsche Montan Technologie, Essen, Germany.

Hartley, J.S. 90 5410 159 8
Drilling: *Tools and programme management*
1994, 25 cm, 192 pp., Hfl.85 / $45.00 / £31
(Student edn., 90 5410 160 1, Hfl.45 / $25.00 / £17)
Types of drills; Rod strings; Holemaking tools; Rock drillability and stability; Downhole drilling problems; Drill hole deviation; Drill-hole deflection; Selection of drilling method for exploration; Preparation for drilling programme; Managing the drilling programme; Downhole surveying; Oriented coring; Downhole logging and inspection; Sampling; Appendices.

All books available from your bookseller or directly from the publisher:
A.A. Balkema Publishers, P.O. Box 1675, Rotterdam, Netherlands
For USA & Canada: A.A. Balkema Publishers, Old Post Rd, Brookfield, VT, USA